

Cellular Constraints to Diffusion

THE EFFECT OF ANTIDIURETIC HORMONE ON WATER FLOWS IN ISOLATED MAMMALIAN COLLECTING TUBULES

JAMES A. SCHAFER and THOMAS E. ANDREOLI

*From the Departments of Medicine (Division of Nephrology) and Physiology,
University of Alabama Medical Center, Birmingham, Alabama 35233*

ABSTRACT These experiments were intended to evaluate the effects of antidiuretic hormone (ADH) on dissipative water transport in cortical collecting tubules isolated from rabbit kidney. In the absence of ADH, the osmotic (P_r , cm sec^{-1}) and diffusional (P_{D_w} , cm sec^{-1}) water permeability coefficients were, respectively, 6 ± 6 and 4.7 ± 1.3 (SD). When ADH was added to the bathing solutions, P_r and P_{D_w} rose to, respectively, 186 ± 38 and 14.2 ± 1.6 (SD). In the absence of ADH, the tubular cells were flat and the lateral intercellular spaces were closed when the perfusing and bathing solutions were, respectively, hypotonic and isotonic; in the presence of ADH, the cells swelled and the intercellular spaces dilated. These data suggest that ADH increased the water permeability of the luminal membranes of the tubules.

It was possible that the ADH-dependent P_r/P_{D_w} ratio was referable to the resistance of the epithelial cell layer (exclusive of luminal membranes) to water diffusion (R_{D_w} , sec cm^{-1}). Such a possibility required that R_{D_w} be ~ 650 , i.e., approximately 25-fold greater than in an equivalent thickness of water. To test this view, it was assumed that R_{D_i} values for lipophilic solutes in lipid bilayer membranes and in luminal membranes were comparable. In lipid bilayer membranes, R_{D_i} was substantially less than 90 sec cm^{-1} for pyridine, *n*-butanol, and 5-hydroxyindole. In renal tubules, R_{D_i} for these solutes ranged from 795 to 2480 with and without ADH. It was assumed that, in the tubules,

R_{D_i} was referable to cellular constraints to diffusion; for these solutes, the latter were 12–25 times greater than in water. Accordingly, it is possible that the ADH-dependent P_r/P_{D_w} ratio was also due to cellular constraints to diffusion.

INTRODUCTION

Certain biological tissues, such as the skin and urinary bladder of amphibians and the collecting tubule of the mammalian kidney, have a primary role in the regulation of water homeostasis. The purpose of this paper is to examine the mode of dissipative water transport across isolated collecting tubule segments from mammalian kidney, and the way in which antidiuretic hormone (ADH)¹ modifies these transport processes.

Ussing and his coworkers (1, 2) first proposed that water traversed aqueous channels in anuran skin, and that ADH increased the size of such pores. The rate of osmotic water flow across anuran skin was considerably greater than might be expected for a diffusion process (1), i.e., the osmotic water permeability coefficient (P_r , cm sec^{-1}) was greater than the diffusional water permeability coefficient (P_{D_w} , cm sec^{-1}); and, ADH increased the P_r/P_{D_w} ratio. Koefoed-Johnsen and Ussing rationalized the difference between P_r and P_{D_w} by assuming that, during osmosis, water traversed membrane pores by laminar flow. By a combined application of Poiseuille's equation and Fick's first law, they computed the effective radii of such pores (1). Hays and Leaf formulated a similar hypothesis to describe the ADH-dependent increase in the water permeability of the toad urinary bladder (3). Arguments

Preliminary reports of this work have appeared in abstract form (37, 38).

Dr. Schafer is an Established Investigator of the American Heart Association. Dr. Andreoli holds a Research Career Development Award from the National Institute of General Medical Sciences.

Received for publication 26 October 1971 and in revised form 26 December 1971.

¹ Abbreviations used in this paper: ADH, antidiuretic hormone; KRB, Krebs-Ringer bicarbonate; KRP, Krebs-Ringer phosphate; THO, tritiated water.

formally identical (4) to that developed by Koefoed-Johnsen and Ussing have been applied to the analysis of P_r/P_{D_w} ratios in a variety of biological and synthetic membranes, including capillaries (5, 6), gastric mucosa (4), the erythrocyte (7), cellophane (8), cellulose (9) and collodion (10) membranes, and lipid bilayer membranes exposed to amphotericin B (11–13).

The permeability of solutes such as urea, thiourea, and acetamide in ADH-treated anuran epithelia (2, 14) is considerably less than might be expected for the restricted diffusion (5, 8) of such molecules through aqueous pores whose radii had been estimated from P_r/P_{D_w} ratios. Accordingly, it was proposed that two series resistances, regulating flows in these tissues, accounted for this discrepancy, i.e., a dense barrier limited the access of certain solutes to an underlying, ADH-sensitive porous barrier, which accounted for the difference between P_r and P_{D_w} (2, 14–16).

The second aspect of the Ussing pore hypothesis was the "solvent drag" effect. Andersen and Ussing first observed that the net flux of solutes such as thiourea or acetamide through isolated frog skin exposed to ADH was increased in proportion to the rate of osmotic volume flow in the same direction; the phenomenon was attributed to coupling of solute flux to solvent flow within aqueous membrane channels (2). Leaf and Hays observed similar effects of volume flow on urea fluxes in the ADH-treated urinary bladder of the toad (14). Subsequently, Kedem and Katchalsky (17, 18) provided quantitative expressions which described the interactions between solute and solvent flows within membranes in terms of the thermodynamics of irreversible processes.

In 1904, Nernst indicated that diffusion-limited liquid layers at phase boundaries could modify reactions between heterogeneous systems (19). Later, Osterhout (20), Jacobs (21), and Teorell (22) noted explicitly the possibility that unstirred layer effects might contribute to the regulation of membrane transport processes. In recent years, a growing body of experimental evidence has accumulated in support of this view. In particular, two factors are noteworthy.

First, unstirred layers may contribute significantly to, and in some instances account entirely for, differences between P_r and P_{D_w} in natural and synthetic membrane systems (11–13, 23–28). In this regard, Dainty and House observed that, in frog skin, the values of P_{D_w} were affected to a considerably greater extent than those of P_r by the magnitude of the unstirred layers (25). Hays, Franki, and Soberman made similar observations on the ADH-treated toad urinary bladder, and showed that the supporting layer of that tissue contributes significantly to the observed resistance to water diffusion, but not to net water flow (29, 30). Second, recent ob-

servations in our laboratory indicate that, in certain instances, osmotic flow-dependent changes in the concentration profiles of solutes at the interfaces between unstirred layers and membranes, rather than the solvent drag phenomenon, may account for changes in the fluxes of solutes across membranes during osmosis (31). Similarly, apparent electrokinetic phenomena in plant cells (32, 33), gall bladder (34, 35), and squid axon (36) may be referable, in part, to perturbations produced by volume flow in the ionic composition of unstirred layers at the membrane interfaces rather than to coupling of ionic and volume flows within membranes. On the basis of such observations, we are skeptical about analyses of water flux data which do not consider explicitly the effects of unstirred layers on transport processes.

This paper presents the results of a series of experiments designed to assess, first, the effects of ADH on the water permeability of isolated, perfused rabbit cortical collecting tubule segments, and second, the permeability of these tubule segments and lipid bilayer membranes to a series of lipophilic solutes. The results are compatible with the view that ADH increases the diffusional flow of water (29) across the luminal plasma membranes of these tubule segments, and that the differences between P_r and P_{D_w} , in this preparation, are referable to constraints imposed on diffusion processes by the epithelial cell layer.

Preliminary reports of some of the observations in this paper have been presented elsewhere (37, 38).

METHODS

The techniques for isolating and perfusing rabbit renal tubule segments have been developed and described with elegance by Burg and his coworkers (39, 40). We have employed these methods, with certain modifications described below.

Isolation and perfusion of tubule segments. With no pretreatment, 1.5–2.5 kg female New Zealand white rabbits were killed by rapid decapitation. A flank incision was opened and the left kidney removed. After stripping off the capsule, a 2–3 mm thick cross-section was cut and transferred to a Petri dish containing a modified Krebs-Ringer bicarbonate buffer (see below) gassed with 95% O_2 –5% CO_2 at ambient temperature. Cortical collecting tubule segments (1.0–4.5 mm) were teased from the slice with fine dissecting forceps. Only the ends of the tubule segments were touched, and these were trimmed subsequently. The isolated tubule segment was transferred in a droplet of the buffer solution to a lucite perfusion chamber (volume \approx 1.2 ml) containing the same medium. The inside and outside diameters of the tubules were, respectively, 22–25 and 35–40 μ . The chamber was thermostatically regulated at 25.0 \pm 0.5°C with a thermoregulator (model 74TA, Yellow Springs Instrument Co., Yellow Springs, Ohio) attached to a heating filament imbedded in the chamber.

The ends of a segment were sucked into glass holding micropipets, and a third concentric perfusing micropipet was advanced from one end into the tubule lumen for a dis-

tance of 100–300 μ . Tubule perfusion, at rates of 10–30 ml min⁻¹, was carried out with a Sage model 255-3 variable speed microsyringe pump (Sage Instruments Inc., White Plains, N. Y.). Liquid silicone rubber (GE RTV 615A) was placed in the tip of the collection pipet (41) to insure a leakproof seal. The perfusion fluid was collected under an oil droplet and removed every 10–15 min with a constant-bore measuring pipet (i.d. $\approx 40 \times 10^{-4}$ cm). For all experiments, the volume of collected fluid was in the range 75–300 nl. The tubule was observed with an inverted microscope (model BR-BMIC, Unitron Instrument Co., Newton Highlands, Mass.) at $\times 50$ –600, and photographs were taken at intervals to record tubule diameter, length, and morphology.

It is particularly relevant in the context of the present experiments to describe the degree of mechanical mixing in the perfusion chamber. In all experiments, the bathing solutions were bubbled continuously with 95% O₂–5% CO₂. As a consequence of the bubbling, the tubule segments oscillated constantly in a vertical direction at rates in the range of 60–270 oscillations/min. The amplitude of the oscillations was in the range of 200–300 μ in the middle of the tubule segments. These oscillations produced stirring which was evident in the vicinity of the tubules. Thus, vigorous convective mixing of minute air bubbles or particles in the bathing solutions was seen uniformly in these experiments, even at distances as close as 2–5 μ to the tubule segments.

Two perfusion solutions were used: (a) An isotonic (290 mOsm liter⁻¹) Krebs-Ringer phosphate (KRP) buffer containing 150 mEq liter⁻¹ NaCl, 2.5 mEq liter⁻¹ K₂HPO₄, 1.0 mEq liter⁻¹ CaCl₂, and 1.2 mEq liter⁻¹ MgSO₄. (b) A hypotonic (125 mOsm liter⁻¹) KRP buffer having the same composition as the isotonic buffer, but containing only 60 mEq liter⁻¹ NaCl. The pH of these solutions was adjusted to 7.4 with 0.1 M HCl. The bathing solutions were: (a) An isotonic (290 mOsm liter⁻¹) Krebs-Ringer bicarbonate (KRB) buffer containing 115 mEq liter⁻¹ NaCl, 25 mEq liter⁻¹ NaHCO₃, 10 mEq liter⁻¹ Na acetate, 1.2 mEq liter⁻¹ NaH₂PO₄, 5 mEq liter⁻¹ KCl, 1 mEq liter⁻¹ CaCl₂, 1.2 mEq liter⁻¹ MgSO₄, and 5.5 mM glucose; 5% (v/v) calf serum (Microbiological Associates, Inc., Bethesda, Md.) was added to this mixture. (b) A hypertonic (455 mOsm liter⁻¹) KRB buffer, identical with isotonic KRB buffer except that it contained 200 mEq liter⁻¹ NaCl. In some experiments (Fig. 5), bathing solutions having osmolalities in the range 190–390 mOsm liter⁻¹ were made by varying the NaCl concentration.

Osmotic volume flow experiments. An osmotic pressure gradient was produced across the tubular epithelium in one of two ways. Either the tubules were perfused with hypotonic KRP, when the bathing phases contained isotonic KRB, or the perfusing solutions were isotonic KRP, when the bathing solutions were hypertonic KRB. The net volume efflux from tubule lumen to bath was determined from the difference between the perfusion rate and the collection rate. In order to measure accurately both the perfusion rate and the rate of leakage from lumen to bath, a radioactive volume marker was added to the perfusion solutions. Two such volume markers were used: inulin-methoxy-³H (New England Nuclear, Boston, Mass., lot Nos. 281-227, 511-200, 511-097; SA, 80-250 mCi/g) at a final activity of 50–100 μ Ci/ml of perfusion solution; or, sucrose-¹⁴C (New England Nuclear, lot Nos. 292-155 and 620-074; SA, 350–500 mCi/mole), at a final activity of 25 μ Ci/ml⁻¹. Under these conditions, we could detect reproducibly rates of leakage

as low as 0.1% of perfusion rate from perfusing to bathing solutions by measuring the appearance of the tagged volume marker in the bathing solutions at 30-min intervals. The leakage rate was less than 1% of the perfusion rate in all the experiments reported in this paper. Accordingly, perfusion rates could be computed directly from the known concentration of volume marker in the initial perfusion fluid and the measured amount of volume marker recovered in the collected fluid.

The measuring pipets had been precalibrated with perfusing solutions to obtain their volume per millimeter. This was an extremely accurate method of calibration, and the mean coefficient of variation for sets of quintuplet calibrations was 0.9%. The rate of volume collection was calculated from the length of the fluid column in the measuring pipet, and the net volume efflux was computed from the difference between the collection and perfusion rates.

In these experiments, hydrostatic pressure differences, if any, were trivial with respect to osmotic pressure differences. Moreover, there was no evident fluid reabsorption in the absence of an osmotic pressure gradient (Table I). Accordingly, J_v , the net volume efflux, may be expressed as (17):

$$J_v = -\sigma_i L_P \Delta\pi, \quad (1)$$

where: J_v (cm³ cm⁻² sec⁻¹) is, to a sufficient approximation, J_w , the net water flow, σ_i is the reflection coefficient (42) of the *i*th solute (used to generate the difference in osmolality between perfusing and bathing solutions), and L_P is the coefficient of hydraulic conductivity (cm sec⁻¹ atm⁻¹). The osmotic pressure difference, $\Delta\pi$, between the bathing and perfusing solutions was computed from the difference between the osmolality of the bathing solution and the antilog of the logarithmic mean of the osmolalities of the initial perfusion fluid and the collected fluid. For comparison with the tracer flux experiments, the results were expressed in terms of an osmotic water permeability coefficient, P_f (cm sec⁻¹), given by (10):

$$P_f = \sigma_i L_P \frac{RT}{\bar{V}_w}, \quad (2)$$

where: R = gas constant, T = absolute temperature, and \bar{V}_w is the partial molar volume of water.

Measurement of diffusional permeability coefficients. In another set of experiments, we measured P_{D_w} (cm sec⁻¹), the permeability coefficient for the diffusion of water, from the unidirectional fluxes of tritiated water (THO) from lumen to bath, either during osmosis or under conditions of zero volume flow in the same tubule segment. We elected to perfuse the tubule segments with 290 mOsm liter⁻¹ KRP, and used either 290 or 455 mOsm liter⁻¹ KRB in the bathing solutions. The perfusing fluids contained 1–1.5 mCi ml⁻¹ THO (New England Nuclear; 100 mCi ml⁻¹, original SA; lot No. 565-010) and 25 μ Ci ml⁻¹ sucrose-¹⁴C.

We wished to prevent equilibration of THO activity between perfusing fluid and bath. Therefore, segments were mounted with only 0.7–1.1 mm of tubule between the perfusing and collecting pipets, in contrast to the 2 to 4.5-mm segments which were used in osmotic flow experiments. Further, the bathing solutions were changed every 30 min. Under these conditions, the THO concentration in the bathing solutions never exceeded 0.1% of the THO activity of the collected solutions. All samples were counted by standard double label techniques in a liquid scintillation counter

(model 3320, Packard Instrument Co., Inc., Downers Grove, Ill.).

When both the perfusing and bathing solutions were isotonic and there was no net volume flow, P_{D_w} was computed from the expression:

$$P_{D_w} = \frac{\dot{V}^{in}}{A_t} \ln \frac{C_w^{in}}{C_w^{out}} \quad (3)$$

where: \dot{V}^{in} = perfusion rate ($\text{cm}^3 \text{sec}^{-1}$), A_t = inner surface area of tubule (cm^2), and C_w^{in} and C_w^{out} are the activities of THO (cpm ml^{-1}), in, respectively, the initial perfusion fluid and the collected fluid. In net volume flow experiments P_{D_w} was computed from the expression:

$$P_{D_w} = \frac{\dot{V}^{in} - \dot{V}^{out}}{A} \left[\frac{\ln(C_w^{in}/C_w^{out})}{\ln(\dot{V}^{in}/\dot{V}^{out})} + \left(\frac{1 + \sigma_i}{2} \right) \right], \quad (4)$$

where \dot{V}^{out} is the collection rate ($\text{cm}^3 \text{sec}^{-1}$), and σ_i is the reflection coefficient of the substance whose permeability is being measured. In the case of water, σ_i is zero by definition. We have included a derivation of equations 3 and 4 in the Appendix because equation 4 differs from that used originally by Grantham and Burg (40).

The same techniques were used to measure P_{D_i} , the diffusional permeability coefficient of the ith solute (cm sec^{-1}). The solute, labeled either with ^3H or ^3H , was added to the perfusion solutions, and the contrasting isotope, either inulin- ^3H or sucrose- ^{14}C , was used as the volume marker. The tracer fluxes were carried out at zero volume flow, and P_{D_i} was computed from equation 3. The solutes included: pyridine- ^3H (Amersham/Searle Corp., (Arlington Heights, Ill.) 158 mCi mmole $^{-1}$, lot No. 7); and *n*-butanol- ^{14}C (New England Nuclear, 2 mCi mmole $^{-1}$, lot No. 318-153).

5-Hydroxyindole was not readily available in labeled form; therefore, fluorescence assays were utilized (43). Specifically, the concentrations of 5-hydroxyindole in the perfusing and bathing solutions used to compute P_{D_i} (equation 3) were determined from fluorescence measurements. The collected samples were ejected from the measuring pipet into 2.0 ml of 0.1 M tris buffer, pH 7.5, and equivalent dilutions of the perfusing solutions were made in the same buffer. The fluorescence of these solutions, at 358 $m\mu$, was measured on an Aminco-Bowman spectrofluorimeter (American Instrument Co., Silver Spring, Md.) which had been peaked for an excitation wave length of 295 $m\mu$.

The relevant observations on the fluorescence measurements are shown in Figs. 1 and 2. The emission peaks of two standard solutions containing 5-hydroxyindole are shown in Fig. 1. In particular, it should be noted that, at an excitation wave length of 295 $m\mu$ and an emission wave length of 358 $m\mu$, it was possible to measure accurately and reproducibly 5-hydroxyindole concentrations as low as 0.04 μM ; all of the experimental samples were in the range 0.5–2 μM . Fig. 2 indicates that, for excitation and emission wave lengths of, respectively, 295 and 358 $m\mu$, the relationship between fluorescence and 5-hydroxyindole concentration, in the range used in these experiments, was linear.

Experiments with lipid bilayer membranes. The techniques for experiments involving lipid bilayer membranes have been presented in detail elsewhere (11, 13, 31), and were used without modification in the present studies. Optically black lipid bilayer membranes separating two aqueous phases were formed by applying lipid solutions with a brush technique (44) to an aperture (1.5–3.0 mm in diameter) in a polyethylene diaphragm (0.125 mm thick) separating

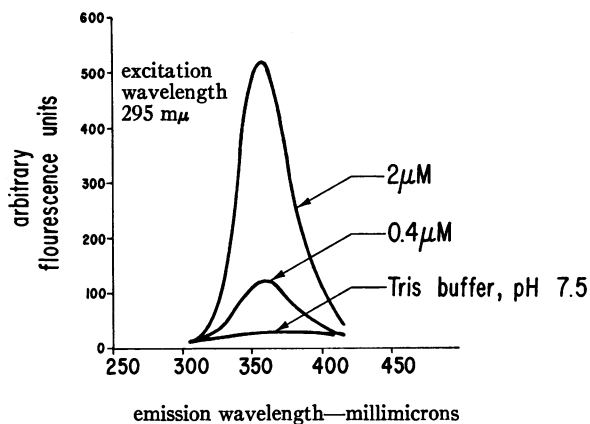


FIGURE 1 The fluorescence emission of 5-hydroxyindole.

two aqueous phases. The lipid solutions used to form membranes (membrane solutions) contained equimolar amounts of cholesterol and phospholipids (extracted from membranes of high potassium sheep red blood cell lipids [45]) dissolved in decane; the total lipid concentration was in the range 25–35 mg/ml. The experiments were carried out in water-jacketed lucite chambers identical with those described previously (11). The “U” tube connecting the two aqueous chambers contained, in earlier experiments (11), a column of oil to insulate the two chambers electrically and isotopically. Since the present experiments involved tracer fluxes of lipophilic solutes, a column of air was also injected into the “U” tube. The electrical properties of the membranes were monitored by a simple voltage clamp apparatus (13). The dc resistances of all of the membranes reported in the present studies were in the range of $10^8 \Omega - \text{cm}^2$.

P_{D_i} (cm sec^{-1}), the permeability coefficient for diffusion of the ith solute, was measured in a manner identical with that described previously (11). Specifically, the aqueous phases bathing the membranes contained equal volumes of identical solutions (indicated in the text) at $25 \pm 0.5^\circ\text{C}$; each aqueous phase was stirred vigorously. The appropriate ^{14}C -labeled isotope was added to one aqueous phase (rear chamber) at a final concentration of approximately 10^7 cpm ml^{-1} . Unidirectional tracer fluxes from one aqueous phase (front chamber) to the other (rear chamber) were carried out for 10–15-min periods. The experimental conditions were

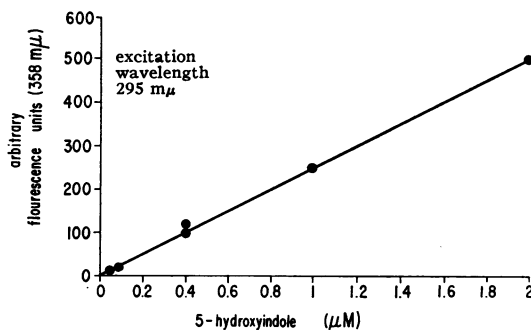


FIGURE 2 The relationship between fluorescence intensity (at 358 $m\mu$) and 5-hydroxyindole concentration.

arranged so that the isotope concentration in the front chamber was negligible (< 1%) during any flux period with respect to the isotope concentration in the rear chamber, which was very nearly constant (11). Accordingly, P_{Di} was computed directly from a modified form of Fick's first law:

$$P_{Di} = \frac{C_{if} \cdot V_f}{C_{ir} \cdot A_m \Delta t} \quad (5)$$

where C_{if}^* and C_{ir}^* are, respectively, the concentration of the *i*th isotope (cpm ml⁻¹) in the front and rear chamber, V_f is the volume of the front chamber (cm³), A_m is the membrane area (cm²) and Δt is the duration of the flux period (sec).

The isotopes used in these experiments were identical with those used in the experiments with renal tubule segments. Measurements of P_{Di} for 5-hydroxyindole in the lipid bilayer membranes were carried out using the fluorescence methods described above.

Reagents. Antidiuretic hormone (ADH; Pitressin, Parke Davis & Company, Detroit, Mich.) when present, was added to the bathing solutions. For radioactive counting, the experimental samples were dissolved in 10 ml of a scintillation solution containing 70 ml Bio-solv 3 solubilizer (Beckman Instruments, Inc., Fullerton, Calif.), 4 g 2,5-diphenyloxazole (PPO), and 0.2 g *p*-bis[2-(5-phenyloxazolyl)] benzene (POPOP) dissolved in 1000 ml toluene. In the experiments with renal tubules, the sample volumes were in the range 150–300 nl. In the lipid bilayer studies, the sample volumes were 0.02–0.05 ml. Dextran (type 60C; average mol wt \approx 77,500) was purchased from Sigma Chemical Co., St. Louis, Mo.

RESULTS

The effect of ADH on water permeability of collecting tubules

The condition for zero volume flow. In accord with earlier observations (40), Table I indicates that, in the absence of osmotic or hydrostatic pressure gradients, there was no significant fluid reabsorption from these collecting tubule segments, either in the presence or absence of ADH. The values of J_w shown in Table I are not significantly different from zero and provide an estimate of the experimental variation in the system.

TABLE I
Zero Volume Flow in Cortical Collecting Tubules

Tubule	Perfusion medium	Bathing medium	ADH	J_w
	mOsm liter ⁻¹		μ U ml ⁻¹	cm ³ sec ⁻¹ cm ⁻² $\times 10^5$
C1	290 KRP	290 KRB	0	+0.26 \pm 0.70 (8)
C36	290 KRP	290 KRB	0	+0.18 \pm 0.22 (11)
	290 KRP	290 KRB	250	+0.12 \pm 0.13 (6)

When present, ADH was added to the bathing solutions. J_w was taken as negative when there was a net water efflux from lumen to bath. The results are expressed as the mean \pm SD for the number of flux periods listed in parentheses.

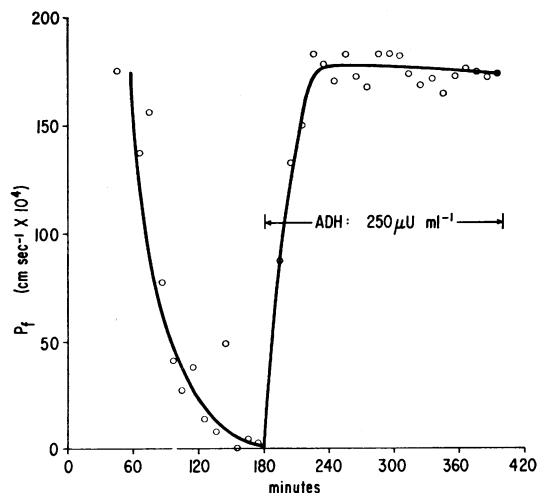


FIGURE 3 The time course of P_t in the absence and presence of ADH.

In this regard, it should be noted that, in other experiments identical with those shown in Table I, negative water flows (lumen to bath), of the same magnitude as those listed in Table I, were noted. Thus, although active Na⁺ and K⁺ transfer occurs in collecting tubule segments (46), it seems unlikely that isotonic fluid reabsorption coupled to active cation transport (47, 48) contributed significantly to the net water flows observed in the present studies.

The effect of ADH on P_t . Fig. 3 summarizes a representative experiment illustrating the effects of ADH on P_t . In the absence of ADH, P_t remained relatively high for approximately 60 min. Subsequently, P_t declined strikingly and approached zero after 140–180 min. Coincident with the decline in osmotic water permeability, the tubular epithelium became flattened and the lateral intercellular spaces were barely visible (Fig. 4, compare 76 and 186 min). It has been suggested that the initial water permeability of collecting tubule segments is referable to endogenous ADH which may be present in the tubules at the time of dissection (40); our experiments provide no additional information regarding this question. When ADH (250 μ U ml⁻¹) was added to the bathing solutions, P_t increased to 175×10^{-4} cm sec⁻¹ and remained constant for at least the next 3 hr (Fig. 3). Concomitantly, the tubular epithelial cells became swollen, their luminal borders bulged, and the lateral intercellular spaces became visible (Fig. 4, 210 min). In other experiments, we have found, in agreement with previous studies (40), that an ADH concentration of approximately 50 μ U ml⁻¹ in the bathing solutions produced a maximal increase in the osmotic water permeability of these tubule segments.

In the absence of ADH, the net water fluxes were much too low to permit an adequate evaluation of the relationship between J_w and $\Delta\pi$, the transtubular osmotic pressure gradient. In the presence of ADH (Fig. 5), J_w was linear, with respect to $\Delta\pi$, in the range 1–6 atm. The differences in the osmolalities of the perfusing and bathing solutions were referable to different NaCl concentrations. Since σ_{NaCl} for these tubule segments, even in the presence of ADH, is unity (36, 37, 52), the σL_p value of 11.0×10^{-6} cm sec⁻¹ atm⁻¹ shown in Fig. 5 (or, in terms of equation 2, $P_f = 150 \times 10^{-4}$ cm sec⁻¹) provides a direct estimate of the ADH-dependent tubular hydraulic conductivity.

Table II summarizes the results of a number of experiments on the effects of ADH on P_f . In the absence of ADH, P_f was computed from osmotic water fluxes in tubules which had been perfused for at least 150 min after decapitation (Fig. 3). The values of P_f ($6 \pm 6 \times 10^{-4}$ cm sec; 15 fluxes) were sufficiently low that the standard deviation, as a percentage of the mean, was comparatively large. Nevertheless, the results show clearly that, in these tubules, ADH increased the value of P_f approximately 30-fold. Further, Table II indicates that the ADH-dependent values of P_f were not significantly different when the perfusing fluids were either hypotonic or isotonic.

These observations (Figs 3, 4; Table II) are both in qualitative and in quantitative accord with the results

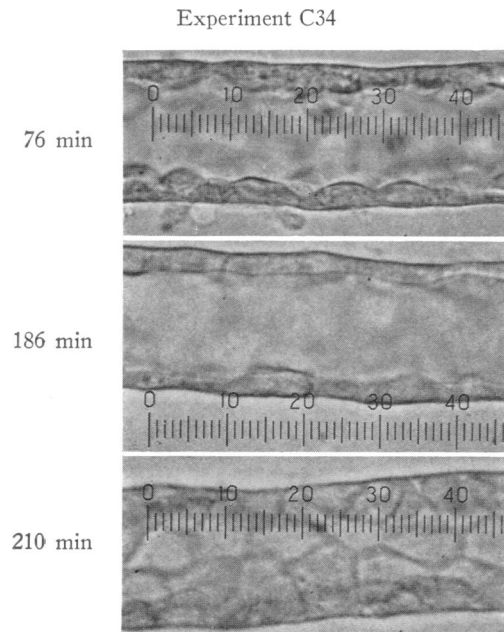


FIGURE 4 Photomicrographs of the collecting tubule from the experiment shown in Fig. 3, taken at 76, 186, and 210 min after decapitation. ($\times 480$ magnification; scale: 2.13μ per division.)

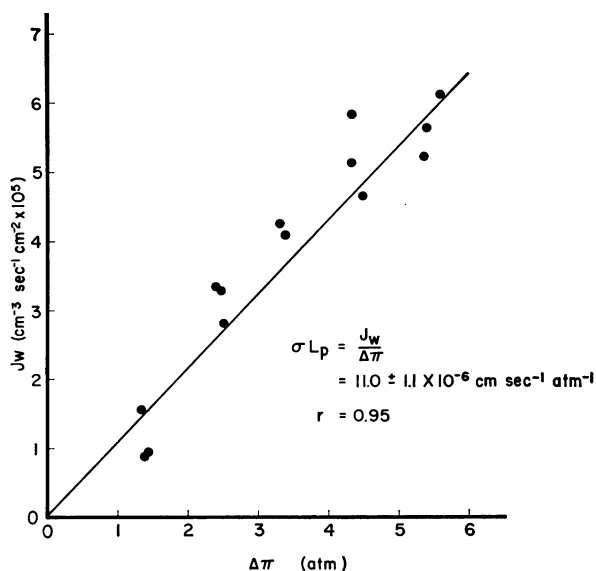


FIGURE 5 The relationship between the transtubular osmotic pressure gradient and net fluid reabsorption. The perfusing solution contained hypotonic KRP buffer ($125 \text{ mOsm liter}^{-1}$) and the bathing solutions contained KRB buffer, in the range $190\text{--}390 \text{ mOsm liter}^{-1}$; ADH ($250 \mu\text{U ml}^{-1}$) was present uniformly in the bathing solutions. σL_p was computed according to equation 1, and the results are expressed as the mean \pm sd. The line was plotted from a least-squares regression of the data (correlation coefficient $r = 0.95$).

obtained previously by Grantham et al. (40, 49–51). In this regard, Grantham et al. have shown by electron microscopy that the changes in tubular morphology which accompany ADH-dependent increases in osmotic water permeability (Fig. 4, 186–210 min) are the result of cellular swelling and widening of the lateral intercellular spaces (50, 51). Thus, the results of the present experiments provide further support for the hypothesis (50, 51) that ADH increases the water per-

TABLE II
The Effect of ADH on P_f during Isotonic or Hypotonic Tubule Perfusion

No. of tubules	Perfusing medium	Bathing medium	ADH	P_f
	mOsm liter^{-1}	mOsm liter^{-1}	$\mu\text{U ml}^{-1}$	$\text{cm sec}^{-1} \times 10^4$
6	125	290	0	6 ± 6 (15)
11	125	290	250	178 ± 34 (83)
7	290	455	250	199 ± 42 (36)
All tubules	—	—	250	186 ± 38 (119)

In all instances, the perfusing and bathing solutions contained, respectively, KRP and KRB buffer at the indicated osmolalities. ADH, when present, was added to the bathing solutions. The results are expressed as the mean \pm sd for the number of flux periods indicated in parentheses.

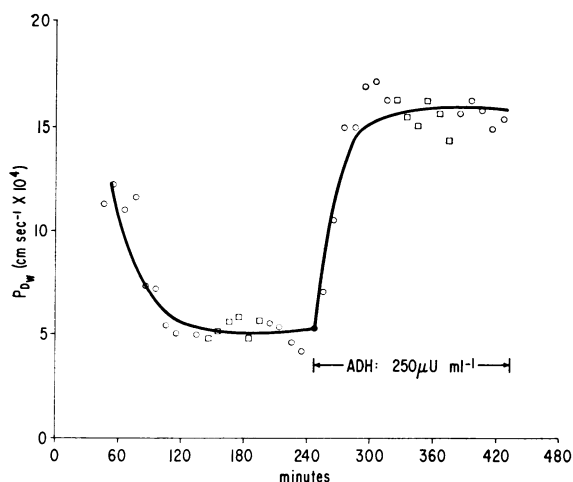


FIGURE 6 The effect of ADH on P_{D_w} . The unidirectional THO fluxes were carried out under the conditions either for zero volume flow (circles) or net osmotic water flow (squares). The perfusing fluid contained 290 mOsm liter⁻¹ KRP in all instances. For zero volume flow experiments (circles), the bathing medium was 290 mOsm liter⁻¹ KRB, and the net water flows were indistinguishable from zero with or without ADH. In the other experiments (squares), the bathing medium was 455 mOsm liter⁻¹ KRB; under these conditions, J_w was indistinguishable from zero without ADH and was $5.5 \pm 1.0 \times 10^{-5}$ cm³ cm⁻²/sec⁻⁴ with ADH.

meability of the luminal interfaces (i.e., plasma membranes and/or tight junctions) of these tubules.

The effect of ADH on P_{D_w} . Fig. 6 illustrates graphically the effect of ADH on P_{D_w} . A comparison of Figs. 3 and 6 indicates that, in the absence of ADH, P_{D_w} declined *pari passu* with P_t . Between approximately 120–240 min, in the absence of ADH, P_{D_w} was in the range of 5×10^{-4} cm sec⁻¹ and remained relatively constant. When ADH ($250 \mu\text{U}^{-1}$ ml⁻¹) was added to the bathing solutions, P_{D_w} rose to approximately 15×10^{-4} cm sec⁻¹. Under these conditions, the values of P_{D_w} remained stable for at least 3 hr and were independent, within experimental error, of the presence or absence of net osmotic water flow (Fig. 6).

Table III summarizes the results of experiments involving P_{D_w} measurements. In three experiments, P_t was measured in the same tubule. The values for P_{D_w} in the absence of ADH, like those for P_t (Table II), were obtained from flux periods carried out at least 150 min after beginning tubule perfusion. From the mean values obtained in seven tubules, it is evident that ADH increased P_{D_w} approximately threefold, i.e., from $4.7 \pm 1.3 \times 10^{-4}$ to $14.2 \pm 1.6 \times 10^{-4}$ cm sec⁻¹. These data are in reasonable agreement with the earlier observations of Grantham and Burg (40).

Effect of viscosity on P_{D_w} . Previous studies from this laboratory, involving lipid bilayer membranes, have

indicated the feasibility of modifying the resistance of unstirred layers, but not membranes, to solute diffusion by varying aqueous phase viscosity with solutes that are excluded from a membrane (13). It was relevant to assess the possible contributions of unstirred layers in the perfusing or bathing solutions to the observed resistance (i.e., $1/P_{D_w}$) to THO diffusion.

In these experiments, dextran (mol wt $\approx 77,500$) was used to vary the viscosity of the perfusing and bathing solutions. Since the reflection coefficient for either NaCl, sucrose, or urea at the luminal interfaces of these tubules is unity (36, 37, 52), both in the presence and absence of ADH, it seemed likely that the dextran added to perfusing solutions would affect only the resistance of those solutions to tracer diffusion. In the case of dextran added to bathing solutions, the problem is more complex. Grantham et al. (51) have shown that horseradish peroxidase (mol wt $\approx 40,000$; [54]) added to bathing solutions may enter the lateral intercellular spaces of cortical collecting tubules and, Welling and Grantham (55) have reported that the reflection coefficient of albumin (mol wt $\approx 60,000$), for the basement membranes of rabbit proximal tubules, is approximately 0.25. In the present experiments, we assumed that the reflection coefficient of dextran at the basement membrane of these tubules was sufficiently high that the dextran-dependent variations in bathing fluid viscosity affected primarily, but perhaps not exclusively, the resistances of these solutions to tracer diffusion.

TABLE III
The Effect of ADH on P_{D_w} in Cortical Collecting Tubules

Tubule	ADH	$P_{D_w,0}$	P_t
	$\mu\text{U ml}^{-1}$	$\text{cm sec}^{-1} \times 10^4$	
Tubules in which P_t and P_D were determined:			
P3	0	4.1 ± 0.1 (7)	—
	250	12.2 ± 4.3 (6)	230 ± 11 (6)
P4	0	3.0 ± 0.3 (4)	—
	250	17.0 ± 1.3 (6)	224 ± 24 (6)
P10	0	4.8 ± 0.4 (7)	—
	250	16.1 ± 1.1 (10)	201 ± 40 (6)
Over-all average for seven tubules:			
	0	4.7 ± 1.3 (35)	—
	250	14.2 ± 1.6 (57)	—

In all instances, the perfusing solutions contained 290 mOsm liter⁻¹ KRP buffer. When P_t was determined, the bathing solutions contained KRB buffer, 455 mOsm liter⁻¹. In all other cases, the bathing solutions contained KRB buffer, 290 mOsm liter⁻¹. When present, ADH was added to the bathing solutions. The results are expressed as the mean \pm SD for the number of flux periods listed in parentheses.

TABLE IV
The Effect of Aqueous Phase Viscosity on P_{D_w}
in Collecting Tubules

Tubule	ADH	Viscosity		P_{D_w}
		Perfusing medium	Bathing medium	
	$\mu U ml^{-1}$	poise $\times 10^3$		$cm sec^{-1} \times 10^4$
P13	250	8.6	9.29	14.37 ± 1.39 (14)
	250	8.6	22.5	13.00 ± 0.43 (7)
P15	250	8.7	9.3	13.10 ± 0.71 (10)
	250	8.7	22.5	13.30 ± 0.56 (6)
P16	—	21.7	9.1	4.58 ± 0.53 (6)
	—	21.7	21.0	4.68 ± 0.68 (6)
	250	21.7	9.1	18.39 ± 1.80 (4)
P17	250	21.7	21.0	17.75 ± 0.87 (5)
	250	94.8	9.1	12.11 ± 0.55 (4)
	250	94.8	96.7	11.21 ± 0.51 (6)

In all instances, the perfusing solutions contained KRP buffer and the bathing solutions contained KRB buffer; both solutions were isotonic (290 mOsm liter⁻¹); the viscosities of these solutions were increased with dextran (mol wt $\approx 77,500$). Solution viscosities were measured with an Ostwald viscometer having an efflux volume of 1.4 ml, in the manner described by Schultz and Solomon (53). The values of P_{D_w} are expressed as the mean \pm SD for the numbers of flux periods indicated in parentheses.

Table IV lists the results of experiments involving four tubules in which P_{D_w} was measured at varying viscosities of the perfusing and bathing solutions. The viscosities of the control solutions were in the range of 9×10^{-3} poise; the bathing solutions, which contained added calf serum, were slightly more viscous than the perfusing solutions (Table IV). The concentrations of dextran used in the experiments varied from 0.5 mM ($\sim 20 \times 10^{-3}$ poise) to 2.0 mM ($\sim 95 \times 10^{-3}$ poise). The values of P_{D_w} , when the perfusing fluid viscosity was 21.7×10^{-3} poise (Table IV, tubule P16), were the same, within experimental error, as the comparable over-all value for P_{D_w} shown in Table III. Further, a comparison of Tables III and IV also indicates that the ADH-dependent values for P_{D_w} , at perfusing fluid viscosities as high as 94.8×10^{-3} poise (Table IV, tubule P17), were only slightly less than the comparable over-all values listed in Table III, and within the experimental range of the individual tubules (P3, P4, P10) listed in Table III. Finally, Table IV shows that, in any particular tubule, increments in bathing fluid viscosity (in the range 22.5 – 96.7×10^{-3} poise) did not modify significantly the values of P_{D_w} .

The permeability of collecting tubules and lipid bilayer membranes to lipophilic solutes

Theoretical. The results in the previous section show that ADH increased the water permeability, and

concomitantly, the P_t/P_{D_w} ratio of the luminal interfaces of the tubules. Such an effect could be dependent on laminar osmotic flow through a porous membrane (1–3). The relationship between volume flow, diffusional flow, and the pore radius is (1, 4, 5, 10, 13):

$$\frac{P_t}{P_{D_w}} = 1 + \frac{r_p^2 RT}{8\eta D_w^0 \nabla_w}, \quad (6)$$

where r_p = pore radius, η = viscosity and D_w^0 = self-diffusion coefficient of water. Table V lists the mean values for the P_t/P_{D_w} ratios with and without ADH, and the corresponding pore radii from equation 6. However, in single membranes containing pores with radii greater than 10 Å, the reflection coefficients of solutes such as urea or sucrose should be less than unity and proportional to solute size (8, 9, 11, 17, 18). In the presence of ADH, NaCl, urea and sucrose have unity reflection coefficients at the luminal interfaces of these tubules (36, 37, 52). Accordingly, a double barrier model, similar to the one proposed for anuran epithelia (1–3, 14–16), would be required if the ADH-dependent P_t/P_{D_w} ratio in these tubules depended on laminar flow in membrane pores (Table V).

The disparity between P_f and P_{D_w} might also be due to diffusion resistances in series with the luminal interfaces (23). This relationship may be expressed as:

$$R_{D_w} = R_\alpha + R_t \quad (7)$$

where R_{D_w} and R_t are, respectively, $1/P_{D_w}$ and $1/P_t$ (23); R_α , the diffusion resistance in series with the luminal interfaces, may be expressed as α/D_w^0 , where α is the thickness of an unstirred layer in which the frictional constraints to diffusion are identical with those in bulk solution (13). Table V lists the values of R_α which were computed from the experimental data and equation 7. For $D_w^0 \approx 2.3 \times 10^{-5}$ cm² sec⁻¹ (56), the corresponding values of α would be 109 μ (without ADH) and 153 μ (with ADH). However, the luminal diameter of the tubules was 22–25 μ (Fig. 4; [50]), and convective mixing of the bathing solutions occurred

TABLE V
The P_f/P_{D_w} Ratio in Collecting Tubules

ADH	P_t	P_{D_w}	P_t/P_{D_w}	r_p	R_α
	$cm sec^{-1} \times 10^4$			Å	$sec cm^{-1}$
—	6	4.7	1.27	1.9	460
+	186	14.2	13.1	12.5	650

The values of P_t and P_{D_w} , are the over-all mean values listed in, respectively, Tables II and III. The values of r_p , the equivalent pore radius, and R_α , the required series resistance, were computed from these data and, respectively, equations 6 and 7.

as close as 2–5 μ from the tubule segments (see Methods). In addition, the values of P_{D_w} , with and without ADH, were relatively independent of perfusing or bathing fluid viscosity, in the range $9\text{--}95 \times 10^{-8}$ poise (Table IV). Accordingly, it is reasonable to assume that bulk phase unstirred layers did not affect significantly the tubular P_t/P_{D_w} ratios.

It is relevant to inquire whether the epithelial cell layer (including cytoplasm, lateral and basilar plasma membranes, lateral intercellular spaces and tubular basement membranes) accounted for the ADH-dependent P_t/P_{D_w} ratio (Table V). Since the thickness of the tubular walls was 6–7 μ (Fig. 4; [50]), such a possibility requires the diffusional resistance of the cell layer, in the presence of ADH, to be 22–25 times greater than that of an equivalent layer of water. This question was evaluated by comparing P_{D_i} for lipophilic solutes in the tubules and in lipid bilayer membranes.

The free diffusion coefficient may be expressed by the Stokes-Einstein relation:

$$D_i^0 = \frac{RT}{6\pi N a_i \eta} \quad (8)$$

where N = Avogadro's number and a_i = radius of i th species. Thus, for bulk unstirred layers in series with a membrane, equation 7 becomes:

$$\frac{1}{P_{D_i}} = \frac{6\pi N a_i}{RT} \eta + \frac{1}{P_{m_i}}, \quad (9)$$

where P_{m_i} is the diffusion permeability coefficient of the membrane for the i th species (13). The slope and intercept of the relationship between $1/P_{D_i}$ and η have been used in this laboratory to assess, respectively, the thickness of unstirred layers in series with lipid bilayer membranes and P_{m_i} for water hydrophilic species such as urea and glycerol (13). Holz and Finkelstein (12) showed that, for *n*-butanol diffusion through bilayer membranes in series with unstirred layers, P_{m_i} was sufficiently great that, for the viscosities η' , η'' , equation 9 reduced to:

$$\frac{R_{D_i}''}{R_{D_i}'} = \frac{\eta''}{\eta'} \quad (10)$$

where $R_{D_i} = 1/P_{D_i}$.

The working hypothesis for the present experiments derives from these observations and the classical work of Overton (57) and Collander and Bärlund (58). Specifically, we assumed that the diffusional resistances of lipid bilayer membranes and the luminal interfaces of collecting tubules to lipophilic solutes were at least comparable. Thus, P_{D_i} determinations in collecting tubules might provide an index of the diffusion resistance of the epithelial cell layer, rather than luminal

interfaces, in the case of solutes whose diffusion through lipid bilayer membranes separating aqueous phases was unstirred layer, rather than membrane-limited (equation 10).

Diffusion of lipophilic solutes in lipid bilayer membranes. The variation of $1/P_{D_i}$ with aqueous phase viscosity may be used to analyze diffusion processes in lipid bilayer membranes separating two aqueous phases (12, 13). The thickness of unstirred layers in series with bilayer membranes, computed from equation 9, was approximately 110 μ (13), under experimental conditions identical with the ones used in the present experiments. This value is in close accord with unstirred layer thicknesses computed by other methods for comparable experimental conditions (12, 26).

Table VI illustrates the effects of varying aqueous phase viscosity on the diffusion permeability coefficients of different lipophilic solutes in these membranes; the solutes tested were pyridine (mol wt = 79.1), *n*-butanol (mol wt = 133.2), and 5-hydroxyindole (mol wt = 133.2). In direct agreement with earlier observations (12), the variation of P_{D_i} with aqueous phase viscosity (Table VI, columns 3 and 4) could be described, within experimental error, by equation 10 (Table VI, columns 5 and 6). Stated in another way, the diffusion resistance of the membranes ($1/P_{m_i}$, equation 9) was negligibly small with respect to the diffusion resistance of the unstirred layers (α/D_i^0) for these solutes. According to this view, it should be possible to compute the unstirred layer thickness directly from the relationship $P_{D_i} = D_i^0/\alpha$ (12); the values of α computed in this manner from the mean control values of P_{D_i} are listed in the last column of Table VI. In each instance, the result was in reasonable agreement with previous estimates of the unstirred layer thickness in this (13) and other (12) laboratories.

The results in Table VI indicate that $1/P_{m_i}$ (equation 9) for those solutes was vanishingly small. In this regard, it has been possible to detect reproducibly, under identical experimental conditions, $1/P_{m_i}$ values as low as 90 sec cm^{-1} , in the case of water (13). Thus, it seems reasonable to assume that the values of $1/P_{m_i}$ for the solutes listed in Table VII were substantially less than 90 sec cm^{-1} . It should be noted in this connection that Lauger, Richter, and Lesslauer (61) have suggested that $1/P_{m_i}$ for the lipophilic species I_2 in similar membranes may be as low as 0.006 sec cm^{-1} .

Diffusion of lipophilic solutes in renal tubules. The permeability coefficients for pyridine, butanol, and 5-hydroxyindole in the renal tubules are shown in Table VII. Several points are noteworthy. First, we observed no change in the morphology of the tubules when these solutes were added to the perfusing solutions. Similarly, concentrations of *n*-butanol in excess of 100 mM did

TABLE VI
The Effect of Viscosity of the Permeability on Lipid Bilayer Membranes to Lipophilic Solutes

Solute	Aqueous phase	η	P_{Di}	η''/η'	R_{Di}''/R_{Di}'	α
		<i>poise</i> $\times 10^3$	<i>cm sec</i> ⁻¹ $\times 10^4$			<i>cm</i> $\times 10^4$
pyridine	0.01 NaCl, 0.01 pyridine	8.8	8.76 \pm 0.82 (6)	—	—	108
	0.01 NaCl, 0.01 pyridine 0.6 sucrose	15.8	5.60 \pm 0.48 (3)	1.80	1.56 \pm 0.39	—
	0.01 NaCl, 0.01 pyridine 0.9 sucrose	24.0	3.30 \pm 0.32 (3)	2.72	2.65 \pm 0.13	—
<i>n</i> -Butanol	0.01 NaCl, 0.01 <i>n</i> -butanol	8.8	8.39 \pm 0.40 (0)	—	—	114
	0.01 NaCl, 0.01 <i>n</i> -butanol 0.7 sucrose	18.9	3.99 \pm 1.30 (15)	2.15	2.10 \pm 0.48	—
5-Hydroxyindole	0.01 NaCl, 0.01 5- hydroxyindole	8.6	5.20 \pm 0.81 (8)	—	—	135
	0.01 NaCl, 0.01 5- hydroxyindole, 0.6 sucrose	16.0	2.40 \pm 0.67 (5)	1.87	2.16 \pm 0.48	—
	0.01 NaCl, 0.01 5- hydroxyindole, 0.9 sucrose	23.5	1.61 (2)	2.75	3.22	—
	0.01 NaCl, 0.01 5- hydroxyindole, 0.0005 dextran	21.0	1.99 \pm 0.21 (4)	2.45	2.61 \pm 0.24	—

The viscosities of the different solutions were measured as described in Table IV. The values of P_{Di} are expressed as the mean \pm SD for the numbers of flux periods in parentheses. The ratios R_{Di}''/R_{Di}' are expressed as the mean \pm SD. The values of α were computed from the relation $P_{Di} = D_i^0/\alpha$. D_i^0 was taken to be: *n*-butanol, 0.96×10^{-5} cm² sec⁻¹ (59); pyridine, 0.95×10^{-5} cm² sec⁻¹ (extrapolated from Longworth {60}); 5-hydroxyindole, 0.7×10^{-5} cm² sec⁻¹ (extrapolated from Longworth {60}).

TABLE VII
The Permeability Coefficients for Lipophilic Solutes in Collecting Tubules

Solute	Perfusing concentration	ADH	Bath viscosity	P_{Di}	R_{Di}	
					Observed	Predicted
					<i>mM</i>	μU ml ⁻¹
Pyridine	15.8	0	9.1	12.6 \pm 1.96 (30)	795	68.2
Pyridine	15.8	0	70.9	14.2 \pm 1.52 (6)	—	—
Pyridine	15.8	250	9.1	13.2 \pm 1.64 (13)	—	—
Butanol	25	0	9.1	12.2 \pm 0.59 (10)	820	67.8
Butanol	25	250	9.1	12.4 \pm 0.62 (9)	—	—
5-Hydroxyindole	20	0	9.0	4.03 \pm 0.54 (11)	2480	92.8
5-Hydroxyindole	20	0	73.2	4.96 \pm 0.45 (4)	—	—
5-Hydroxyindole	20	250	9.0	3.94 \pm 0.66 (12)	—	—

The perfusing and bathing solutions contained, respectively, KRP and KRB buffer; both solutions were isotonic (290 mOsm liter⁻¹). The indicated concentrations of the test solutes were added to the perfusing solutions. ADH, when present, was added to the bathing solutions. The viscosity of the bathing solutions was increased with dextran (1.5 mM). P_{Di} is expressed as the mean \pm SD for the number of flux periods listed in parentheses; each experimental condition involved measurements on two tubules. The observed values of R_{Di} are the mean values of $1/P_{Di}$. The predicted values of R_{Di} were computed for the free diffusion of the test solutes through a 6 μ thick layer of water, using the values of D_i^0 listed in Table VI.

not affect significantly the ADH-dependent osmotic water permeability properties of the tubules (52). Second, the control ($\eta = 9 \times 10^{-8}$ poise; no ADH) P_{D_1} values of pyridine and butanol were approximately the same, and greater than P_{D_1} for 5-hydroxyindole, in qualitative agreement with the D_1^0 values for these solutes and with the results in lipid bilayer membranes (Table VI). Third, ADH did not affect P_{D_1} for any of the solutes tested. Similarly, the permeability coefficients of pyridine and 5-hydroxyindole were not changed significantly when the bathing solution viscosity was increased approximately ninefold. These observations suggest that the diffusion of these solutes through the tubule walls was not primarily dependent either on hydrophilic sites in the luminal interfaces or on unstirred layers in the bathing solutions. Finally, it is instructive to compare the diffusion of these solutes through the tubules and in water. The observed values for R_{D_1} in Table VII are the mean values of $1/P_{D_1}$. The predicted values of R_{D_1} were computed for the relation $\Delta x/D_1^0$, where Δx was taken to be 6.5μ , the mean thickness of the tubules used in these experiments. From Table VII, the ratios of the observed to predicted values of R_{D_1} were 11.6, 12.2, and 27 for, respectively, pyridine, butanol, and 5-hydroxyindole. Stated in another way, the resistance of these tubules to the diffusion of these solutes was, at a minimum, 10-fold greater than that of an equivalent thickness of water.

DISCUSSION

The experiments described in this paper indicate that ADH increases the osmotic (Tables II and V; Figs. 3, 4) and diffusional (Tables III and V; Fig. 6) flow

of water across the luminal interfaces of these cortical collecting tubules. Our results in this regard are in close agreement with the original observations of Grantham et al. (40, 49–51). Table VIII summarizes some relevant observations from the literature on the effects of ADH on P_f and P_{D_w} in distal and collecting tubules in mammalian kidney. It is clear that in each instance, the pattern of response to ADH, with respect to P_f , P_{D_w} and the P_f/P_{D_w} ratio is similar. Presumably, the observed variation in the values of these coefficients relate to species differences, site differences, differences in technique, or some combination of these factors.

In regard to the values of P_f , it should be noted that the lateral intercellular spaces of some epithelia, such as the gall bladder (34, 35, 65), are effective unstirred layers. Grantham, Ganote, Burg, and Orloff have suggested that, in isolated collecting tubules exposed to ADH, a portion of osmotic volume flow occurs through the lateral intercellular spaces (51). Thus, the possibility exists that the "sweeping-away" effect of osmotic water flow in the lateral intercellular spaces reduced the salt concentration and accordingly, the osmotic pressure gradient across the luminal interfaces (23, 32–35, 66). Under these conditions, the observed values of P_f would provide an incorrectly low estimate of L_p .

In this connection, if two solutions (I and II) are separated by a membrane, the relationship between the i th solute concentration in bulk phase II (C_i^{bII}) and an unstirred layer α II ($C_i^{\alpha II}$), during volume flow from I to II is (23, 25):

$$C_i^{\alpha II} = C_i^{bII} \exp. - (J_w R_{\alpha II}), \quad (11)$$

where J_w is the volume flow ($\text{cm}^3 \text{cm}^{-2} \text{sec}^{-1}$) and $R_{\alpha II}$

TABLE VIII
The Effect of ADH on P_f and P_{D_w} in Mammalian Kidney

Site	Species	Technique	P_f		P_{D_w}		Ref.
			-ADH	+ADH	-ADH	+ADH	
<i>cm sec⁻¹ × 10⁴</i>							
Medullary collecting duct	Rat	Microperfusion, intact kidney	39	208	4.5	8.7	62
Cortical distal tubule	Rat	Microperfusion, intact kidney	217	829	15.7	32.7	63
Cortical distal tubule	Rat	Microperfusion, intact kidney	103	1030	—	—	64
Cortical collecting tubule	Rabbit	Isolated tubule	8–37	157–185	3.8	9.7	40, 49

The values of P_f and P_{D_w} were derived from the data cited in the references.

is the diffusional resistance ($\alpha II/D_1^0$) of the unstirred layer. Equation 11 indicates that C_1^{int} will be reduced in exponential relationship to both J_w and R_{int} . In the present experiments, the ADH-dependent value of L_p , and accordingly P_r , was constant over at least a six-fold range of water flows (Fig. 5). Secondly, the ADH-dependent values of P_r were not significantly different during hypotonic or isotonic perfusion (Table II). However, it is likely that the diffusional resistance of the lateral intercellular spaces varied under these conditions, since the latter are dilated during hypotonic perfusion (Fig. 4; [50]) and closed during isotonic perfusion² (50). Taken together, these observations suggest that, in these tubules, the concentrations of solutes in the lateral intercellular spaces during osmosis may not have been reduced sufficiently to affect significantly the values of P_r . Clearly, an explicit answer to this question will require both different experimental techniques and more precise characterization of solute diffusion processes in the lateral intercellular spaces.

The experiments with lipid bilayer membranes in series with unstirred layers (Table VI), in agreement with the observations of Holz and Finkelstein (12), indicate that, to a reasonable approximation, equation 10, rather than equation 9, characterized the diffusion of the lipophilic solutes pyridine, *n*-butanol, and 5-hydroxyindole. As indicated previously (see Results), it is likely that $1/P_m$ for these solutes in the lipid bilayer membranes was substantially less than 90 sec cm^{-1} . Thus, to the extent that lipid bilayer membranes provide a frame of reference for evaluating the permeability of the luminal interfaces of the collecting tubules to these lipophilic solutes, a comparison of the results in Tables VI and VII indicates that the diffusional resistance of the tubules to pyridine, *n*-butanol, and 5-hydroxyindole was referable to the epithelial cell layer, rather than to the luminal interfaces. Further, it is evident from Table VII that R_{D_1} for these solutes was 12 (pyridine and butanol) to 25 times greater than predicted for an equivalent layer of water. On the basis of these observations, we suggest that the diffusional resistance of the epithelial cell layer to water diffusion might also be substantially greater than that of an equivalent layer of water. In this regard, several conditions are noteworthy.

First, the origin of the increased diffusional resistance of the epithelial cell layer with respect to water might relate, in principle, to greater frictional constraints to diffusion, to a reduced area per unit path length or to a combination of these factors. Both Fenchel and Horowitz (67) and Dick (68) have indicated

² Schafer, J. A., and T. E. Andreoli, unpublished observations.

that cytoplasmic viscosity, among other factors, may impede to a striking degree the diffusion of THO (68) and other small molecules (e.g., *n*-butanol and thiourea [67]). Alternatively, it may be that diffusing species such as water, pyridine, *n*-butanol, and 5-hydroxyindole traverse selective, restricted pathways in cell cytoplasm or in the lateral intercellular spaces. The present experiments provide no information which distinguishes among these possibilities.

Second, the observed value of R_{D_1} for 5-hydroxyindole was 25 times greater than predicted for an equivalent layer of water (Table VII). If it is assumed that the cellular constraints to water diffusion were equally great, the latter would account entirely for the ADH-dependent P_r/P_{D_w} ratio in these tubules (Table V). However, the ratio of the observed to predicted values of R_{D_1} for pyridine and butanol were approximately 12. If comparable constraints applied to water diffusion, R_{D_w} for an epithelial cell layer 6.5μ thick would be 340 sec cm^{-1} , in contrast to the value of 650 sec cm^{-1} predicted from the ADH-dependent P_r/P_{D_w} ratio (Table V). It may be that the cellular restrictions to diffusion of pyridine and *n*-butanol were less than for water. In this connection, it is noteworthy that the factors regulating diffusion of molecules in cytoplasm are multiple, and involve, at a minimum, molecular size, lipid solubility, hydrogen-bonding capability, and the organization of protein structure in cytoplasm (67, 68). Recognizing these complexities, we suggest the possibility that the resistance of the epithelial cell layer to the diffusion of water may account entirely for the ADH-dependent P_r/P_{D_w} ratio in these tubules. According to this view, the effects of ADH on the water permeability of these tubules may be rationalized entirely in terms of a diffusion process, in accord with the hypothesis of Hays, Franki, and Soberman (29-30) for the action of the hormone on the luminal membranes of the toad urinary bladder. Similarly, cellular constraints to diffusion may also account for the observed disparity between P_r and P_{D_w} in the absence of ADH (Table V). However, the range of P_r values without ADH is comparatively large (Table II); accordingly, the value of R_α computed for this condition (Table V) represents an approximation.

Finally, it is reasonable to inquire about the extent to which the permeability of pyridine, *n*-butanol, and 5-hydroxyindole in lipid bilayer membranes provides an adequate frame of reference for evaluating the transport of these species in luminal interfaces. The assumption derives from the classical observations of Overton (57) and Collander and Bärlund (58) on the high degree of correlation between lipid solubility and membrane permeability for relatively small molecular species. With few exceptions, more recent studies have

affirmed this relationship (69). In this regard, it is clear that the values of P_{D_1} for pyridine, *n*-butanol, and 5-hydroxyindole in these tubules were independent of ADH (Table VII), and presumably, of the presence of hydrophilic sites in luminal interfaces. Further, the architecture proposed for lipid bilayer membranes (70, 71) is quite similar to that proposed to be the fundamental structural unit for most biological membranes (72). Thus, although no definitive answer to the question is possible, the assumption seems at least plausible.

APPENDIX

The purpose of this section is to derive equations 3 and 4, since the latter, used in this paper to compute P_{D_w} during osmotic volume flow in the experiments with tubule segments, differs from that used originally by Grantham and Burg (40). The formulation of the problem is illustrated schematically in Fig. 7. The tubule segment is treated as a uniform right circular cylinder having length L and radius r . At the origin of the segment ($x = 0$), the tubule is perfused at a rate \dot{V}^{in} with fluid containing the *i*th solute at a concentration C_i^{in} . At $x = L$, fluid containing solute at a concentration C_i^{out} is collected at a rate \dot{V}^{out} . The concentration of solute in the bath is C_i^b ; as noted earlier, (see Results), C_i^b in these experiments was less than 0.1% of C_i^{out} .

Consider an infinitely thin fluid lamella of thickness dx within the tubule lumen. The rate of entry of the *i*th solute into dx is $\dot{V}^x C_i^x$, where C_i^x and \dot{V}^x are, respectively, solute concentration and volume flow rate at x . The rate of exit of the *i*th solute is $\dot{V}^{x+dx} C_i^{x+dx} + J_i$, where C_i^{x+dx} and \dot{V}^{x+dx} are, respectively, solute concentration and volume flow rate at $(x + dx)$, and J_i is the solute flux, lumen to bath. In the steady state, the equation of continuity for dx is:

$$\dot{V}^x C_i^x = \dot{V}^{x+dx} C_i^{x+dx} + J_i. \quad (A1)$$

Since dx is an infinitely thin segment, we assume that $C^x \approx C^{x+dx}$. Accordingly, following Kedem and Katchalsky (17), the dissipative transport of the *i*th species from the lumen to bath may be described by the expression:

$$J_i = P_{D_i} A_x (C_i^x - C_i^b) + J_v (1 - \sigma_i) \bar{C}_i, \quad (A2)$$

where J_v is the volume flow from lumen to bath, A_x is the area of the lamella dx , and \bar{C}_i is, to a sufficient approximation (17):

$$\bar{C}_i = \frac{C_i^x + C_i^b}{2}. \quad (A2a)$$

For the lamella dx , J_v is given by $(\dot{V}^x - \dot{V}^{x+dx})$, and A_x is

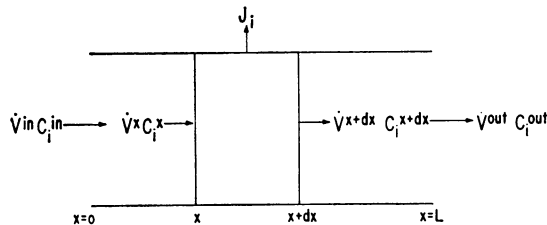


FIGURE 7 Schematic diagram of a collecting tubule segment as a uniform right circular cylinder having radius r and length L .

$2\pi r dx$. Since C_i^b is negligibly small with respect to C_i^x , substitution of equations A2 and A2a into A1 yields:

$$\dot{V}^x C_i^x = \dot{V}^{x+dx} C_i^{x+dx} + P_{D_i} 2\pi r dx C_i^x + (\dot{V}^x - \dot{V}^{x+dx}) \frac{(1 - \sigma_i)}{2} C_i^x \quad (A3)$$

Expanding the terms in equation A3 with a Taylor series, and neglecting differentials higher than first order, we have:

$$\dot{V}^x \frac{dC_i^x}{dx} + P_{D_i} 2\pi r C_i^x + C_i^x \left(\frac{1 + \sigma_i}{2} \right) \frac{d\dot{V}^x}{dx} = 0 \quad (A4)$$

Consider the case where net volume flow, and consequently $d\dot{V}^x/dx$, are zero. In this instance, \dot{V}^x is a constant term, \dot{V}^{in} , and equation A4 becomes:

$$\frac{dC_i^x}{C_i^x} = - \frac{2\pi r P_{D_i}}{\dot{V}^{in}} dx. \quad (A5)$$

Integrating equation A5 between $x = 0$ and $x = L$, we have:

$$P_{D_i} = \frac{\dot{V}^{in}}{A_t} \ln \frac{C_i^{in}}{C_i^{out}}, \quad (A6)$$

which is equation 3 in the text.

For the case where net volume flow occurs, we assume that the rate of fluid reabsorption from the tubule lumen is sufficiently small that $d\dot{V}^x/dx$ may be described, to a sufficient approximation, by the expression:

$$\frac{d\dot{V}^x}{dx} \approx \frac{\dot{V}^{out} - \dot{V}^{in}}{L} = K, \quad (A7)$$

where K is a constant (It can be shown that the approximation in equation A7 is quite reasonable for those cases where $\dot{V}^{out} \geq 0.5\dot{V}^{in}$, a condition which obtains in the present experiments (Table I). Substituting equation A7 into equation A4 and rearranging, we have:

$$\frac{dC_i^x}{C_i^x} = \left[\frac{P_{D_i} 2\pi r + \left(\frac{1 + \sigma_i}{2} \right) K}{\dot{V}^x} \right] dx. \quad (A8)$$

In view of equation A7, \dot{V}^x may be described by:

$$\dot{V}^x = \dot{V}^{in} + Kx. \quad (A9)$$

Substituting equation A9 into equation A8 and rearranging, we have:

$$\int_{x=0}^{x=L} \frac{dC_i^x}{C_i^x} = - \left[P_{D_i} 2\pi r + \left(\frac{1 + \sigma_i}{2} \right) K \right] \int_{x=0}^{x=L} \frac{dx}{\dot{V}^{in} + Kx} \quad (A10)$$

The integrated form of equation A10 is:

$$\ln \frac{C_i^{in}}{C_i^{out}} = \left[\frac{P_{D_i} 2\pi r}{K} + \left(\frac{1 + \sigma_i}{2} \right) \right] \ln \left(\frac{\dot{V}^{in} + KL}{\dot{V}^{in}} \right). \quad (A11)$$

Substituting for K from equation A7 and rearranging, we have:

$$P_{D_i} = \frac{\dot{V}^{in} - \dot{V}^{out}}{A_t} \left[\frac{\ln(C_i^{in}/C_i^{out})}{(\dot{V}^{in}/\dot{V}^{out})} + \left(\frac{1 + \sigma_i}{2} \right) \right], \quad (A12)$$

which is equation 4 in the text. This expression differs from that used by Grantham and Burg in the $\left(\frac{1 + \sigma_i}{2}\right)$ term. However, the latter is usually small in comparison to the logarithmic term in brackets. Accordingly, we expect our results to be comparable to those of Grantham and Burg (40). Lastly, it should be noted that, in the case of zero fluid reabsorption, equation A12 reduces directly to equation A6 by the application of L'Hospital's rule.

ACKNOWLEDGMENTS

We are grateful to our research assistants S. L. Troutman and M. L. Watkins for their able assistance in carrying out these experiments.

This work was supported by research grants from the National Institutes of Health (AM-14873), National Science Foundation (GB-8479), and American Heart Association (70-1047).

REFERENCES

1. Koefoed-Johnsen, V., and H. H. Ussing. 1953. The contributions of diffusion and flow to the passage of D₂O through living membranes. *Acta Physiol. Scand.* **28**: 60.
2. Andersen, B., and H. H. Ussing. 1957. Solvent drag on non-electrolytes during osmotic flow through isolated toad skin and its response to antidiuretic hormone. *Acta Physiol. Scand.* **39**: 228.
3. Hays, R. M., and A. Leaf. 1962. Studies on the movement of water through the isolated toad bladder and its modification by vasopressin. *J. Gen. Physiol.* **45**: 905.
4. Durbin, R. P., H. Frank, and A. K. Solomon. 1956. Water flow through frog gastric mucosa. *J. Gen. Physiol.* **39**: 535.
5. Pappenheimer, J. R., E. M. Renkin, and L. M. Borrero. 1951. Filtration, diffusion and molecular sieving through peripheral capillary membranes. *Amer. J. Physiol.* **167**: 13.
6. Pappenheimer, J. R. 1953. Passage of molecules through capillary walls. *Physiol. Rev.* **33**: 387.
7. Paganelli, C. V., and A. K. Solomon. 1957. The rate of exchange of tritiated water across the human red cell membrane. *J. Gen. Physiol.* **41**: 259.
8. Renkin, E. M. 1955. Filtration, diffusion, and molecular sieving through porous cellulose membranes. *J. Gen. Physiol.* **38**: 225.
9. Durbin, R. P. 1960. Osmotic flow of water across permeable cellulose membranes. *J. Gen. Physiol.* **44**: 315.
10. Robbins, E., and A. Mauro. 1960. Experimental study of the independence of diffusion and hydrodynamic permeability coefficients in collodion membranes. *J. Gen. Physiol.* **43**: 523.
11. Andreoli, T. E., V. W. Dennis, and A. M. Weigl. 1969. The effect of amphotericin B on the water and non-electrolyte permeability of thin lipid membranes. *J. Gen. Physiol.* **53**: 133.
12. Holz, R., and A. Finkelstein. 1970. The water and non-electrolyte permeability induced in thin lipid membranes by the polyene antibiotics nystatin and amphotericin B. *J. Gen. Physiol.* **56**: 125.
13. Andreoli, T. E., and S. L. Troutman. 1971. An analysis of unstirred layers in series with "tight" and "porous" lipid bilayer membranes. *J. Gen. Physiol.* **57**: 464.
14. Leaf, A., and R. M. Hays. 1962. Permeability of the isolated toad bladder to solutes and its modification by vasopressin. *J. Gen. Physiol.* **45**: 921.
15. Lichtenstein, N. S., and A. Leaf. 1965. Effect of amphotericin B on the permeability of the toad bladder. *J. Clin. Invest.* **44**: 1328.
16. Lichtenstein, N. S., and A. Leaf. 1966. Evidence for a double series permeability barrier at the mucosal surface of the toad bladder. *Ann. N. Y. Acad. Sci.* **137**: 556.
17. Kedem, O., and A. Katchalsky. 1958. Thermodynamic analysis of the permeability of biological membranes to nonelectrolytes. *Biochim. Biophys. Acta.* **27**: 229.
18. Kedem, O., and A. Katchalsky. 1961. A physical interpretation of the phenomenological coefficients of membrane permeability. *J. Gen. Physiol.* **45**: 143.
19. Nernst, W. 1904. Theorie der Reaktionsgeschwindigkeit in heterogenen Systemen. *Z. Phys. Chem.* **47**: 52.
20. Osterhout, W. J. V. 1933. Permeability in large plant cells and in models. *Ergeb. Physiol. Biol. Chem. Exp. Pharmakol.* **35**: 967.
21. Jacobs, M. H. 1935. Diffusion processes. *Ergeb. Biol.* **12**: 1.
22. Teorell, T. 1936. A method for studying conditions within diffusion layers. *J. Biol. Chem.* **133**: 735.
23. Dainty, J. 1963. Water relations of plant cells. *Advan. Bot. Res.* **1**: 279.
24. Ginzburg, B. Z., and A. Katchalsky. 1963. The frictional coefficients of the flows of non-electrolytes through artificial membranes. *J. Gen. Physiol.* **47**: 403.
25. Dainty, J., and C. R. House. 1966. "Unstirred layers" in frog skin. *J. Physiol. (London)*. **182**: 66.
26. Cass, A., and A. Finkelstein. 1967. Water permeability of thin lipid membranes. *J. Gen. Physiol.* **50**: 1765.
27. Gutknecht, J. 1967. Membranes of *Valonia ventricosa*: apparent absence of water-filled pores. *Science (Washington)*. **158**: 787.
28. Everitt, C. T., W. R. Redwood, and D. A. Haydon. 1969. The problem of boundary layers in the exchange of water across bimolecular lipid membranes. *J. Theor. Biol.* **22**: 20.
29. Hays, R. M., and N. Franki. 1970. The role of water diffusion in the action of vasopressin. *J. Membrane Biol.* **2**: 263.
30. Hays, R. M., N. Franki, and R. Soberman. 1971. Activation energy for water diffusion across the toad bladder: evidence against the pore enlargement hypothesis. *J. Clin. Invest.* **50**: 1016.
31. Andreoli, T. E., J. A. Schafer, and S. L. Troutman. 1971. Coupling of solute and solvent flows in porous lipid bilayer membranes. *J. Gen. Physiol.* **57**: 479.
32. Barry, P. H., and A. B. Hope. 1969. Electroosmosis in membranes: effects of unstirred layers and transport numbers. I. Theory. *Biophys. J.* **9**: 700.
33. Barry, P. H., and A. B. Hope. 1969. Electroosmosis in membranes: effects of unstirred layers and transport numbers. II. Experimental. *Biophys. J.* **9**: 729.
34. Wedner, H. J., and J. M. Diamond. 1969. Contributions of unstirred layer effects to apparent electrokinetic phenomena in the gall bladder. *J. Membrane Biol.* **1**: 92.
35. Machen, T. E., and J. M. Diamond. 1969. An estimate of the salt concentration in the lateral intercellular spaces of rabbit gall bladder during maximal fluid transport. *J. Membrane Biol.* **1**: 194.

36. Vargas, F. F. 1968. Water flux and electrokinetic phenomena in the squid axon. *J. Gen. Physiol.* 51: 1235.
37. Schafer, J. A., and T. E. Andreoli. 1970. Vasopressin-dependent reflection coefficients in isolated collecting tubules. *Physiologist.* 13: 302.
38. Schafer, J. A., and T. E. Andreoli. 1971. The effects of vasopressin on water and solute permeability in isolated perfused collecting tubules. Abstracts and Programs of the Biophysical Society 15th Annual Meeting. New Orleans, La. 278a.
39. Burg, M., J. Grantham, M. Abramow, and J. Orloff. 1966. Preparation and study of fragments of single rabbit nephrons. *Amer. J. Physiol.* 210: 1293.
40. Grantham, J. J., and M. B. Burg. 1966. Effect of vasopressin and cyclic AMP on permeability of isolated collecting tubules. *Amer. J. Physiol.* 211: 255.
41. Burg, M., S. Helman, J. Grantham, and J. Orloff. 1970. Effect of vasopressin on the permeability of isolated rabbit cortical collecting tubules to urea, acetamide and thiourea. In *Urea and the Kidney*. Bodil Schmidt-Nielsen, editor. Excerpta Medica Foundation, Amsterdam. 193.
42. Staverman, A. J. 1951. The theory of measurement of osmotic pressure. *Rec. Trav. Chim. Pays-Bas.* 70: 344.
43. Bean, R. C., W. C. Shepherd, and H. Chan. 1968. Permeability of lipid bilayer membranes to organic solutes. *J. Gen. Physiol.* 52: 495.
44. Mueller, P., O. Rudin, H. Ti Tien, and W. C. Westcott. 1962. Reconstitution of excitable cell membrane structure in vitro. *Circulation.* 26: 1167.
45. Andreoli, T. E., and M. Monahan. 1968. The interaction of polyene antibiotics with thin lipid membranes. *J. Gen. Physiol.* 52: 300.
46. Grantham, J. J., M. B. Burg, and J. Orloff. 1970. The nature of transtubular Na and K transport in isolated rabbit renal collecting tubules. *J. Clin. Invest.* 49: 1815.
47. Diamond, J. M. 1964. The mechanism of isotonic water transport. *J. Gen. Physiol.* 48: 15.
48. Burg, M. B., and J. Orloff. 1968. Control of fluid absorption in the renal proximal tubule. *J. Clin. Invest.* 47: 2016.
49. Grantham, J. J., and J. Orloff. 1968. Effect of prostaglandin E₁ on the permeability response of the isolated collecting tubule to vasopressin, adenosine 3',5'-monophosphate, and theophylline. *J. Clin. Invest.* 47: 1154.
50. Ganote, C. E., J. J. Grantham, H. L. Moses, M. B. Burg, and J. Orloff. 1968. Ultrastructural studies of vasopressin effect on isolated perfused renal collecting tubules of the rabbit. *J. Cell Biol.* 36: 355.
51. Grantham, J. J., C. E. Ganote, M. B. Burg, and J. Orloff. 1968. Paths of transtubular water flow in isolated renal collecting tubules. *J. Cell Biol.* 41: 562.
52. Schafer, J. A., and T. E. Andreoli. 1972. The effect of antidiuretic hormone on solute flows in mammalian collecting tubules. *J. Clin. Invest.* 51: 1279.
53. Schultz, S. G., and A. K. Solomon. 1961. Determination of the effect hydrodynamic radii of small molecules by viscometry. *J. Gen. Physiol.* 44: 1189.
54. Graham, R. C., and M. J. Karnovsky. 1966. Glomerular permeability. Ultrastructural cytochemical studies using peroxidases as protein tracers. *J. Exp. Med.* 124: 1123.
55. Welling, L. W., and J. J. Grantham. 1971. Effect of albumin on transmembrane water flow. *Clin. Res.* 19: 553P.
56. Wang, J. H., C. V. Robinson, and I. S. Edelman. 1953. Self-diffusion and structure of liquid water. III. Measurement of the self-diffusion of liquid water with H³, H³ and O¹⁸ as tracers. *J. Amer. Chem. Soc.* 75: 466.
57. Overton, E. 1902. Beiträge zur allgemeinen Muskel- und Nerven-physiologie. *Pflüegers Arch. Gesamte Physiol. Menschen. Tiere.* 92: 115.
58. Collander, R., and H. Bärlund. 1933. Permeabilitätsstudien an Chara ceratophylla. II. Die Permeabilität für Nicht electrolyte. *Acta Bot. Fenn.* 11: 1.
59. Lyons, P. A., and C. L. Sandquist. 1953. A study of the diffusion of n-butyl alcohol in water using the Gouy interference method. *J. Amer. Chem. Soc.* 75: 3896.
60. Longsworth, L. G. 1953. Diffusion measurements, at 25°, of aqueous solutions of amino acids, peptides and sugars. *J. Amer. Chem. Soc.* 75: 5705.
61. Läger, P., J. Richter, and W. Lesslauer. 1967. Electrochemistry of bimolecular phospholipid membranes. I. Impedence measurements in aqueous iodine solutions. *Ber. Bunsenges. Phys. Chem.* 71: 906.
62. Morgan, T., and R. W. Berliner. 1968. Permeability of the loop of Henle, vasa recta, and collecting duct to water, urea and sodium. *Amer. J. Physiol.* 215: 108.
63. Persson, E. 1970. Water permeability in rat distal tubules. *Acta Physiol. Scand.* 78: 364.
64. Ullrich, K. J., G. Rumrich, and G. Fuchs. 1964. Wasserpermeabilität und transtubulärer Wasserfluss corticaler Nephronabschnitte bei verschiedenen Diuresezuständen. *Pflüegers Arch. Gesamte Physiol. Menschen. Tiere.* 280: 99.
65. Diamond, J. M., and W. H. Bossert. 1967. Standing gradient osmotic flow. A mechanism for coupling of water and solute transport in epithelia. *J. Gen. Physiol.* 50: 2061.
66. Heyer, E., A. Cass, and A. Mauro. 1969. A demonstration of the effect of permeant and impermeant solutes, and unstirred boundary layers on osmotic flow. *Yale J. Biol. Med.* 42: 139.
67. Fenichel, I. R., and S. B. Horowitz. 1963. The transport of non-electrolytes in muscle as a diffusional process in cytoplasm. *Acta Physiol. Scand.* 60: 1s.
68. Dick, D. A. T. 1964. The permeability coefficient of water in the cell membrane and the diffusion coefficient in the cell interior. *J. Theor. Biol.* 7: 504.
69. Wright, E. M., and J. M. Diamond. 1969. Patterns of non-electrolyte permeability. *Proc. Roy. Soc. Ser. B.* 172: 227.
70. Henn, F. A., G. L. Decker, J. W. Greenawalt, and T. E. Thompson. 1967. Properties of lipid bilayer membranes separating two aqueous phases: electron microscope studies. *J. Membrane Biol.* 24: 51.
71. Henn, F. A., and T. E. Thompson. 1968. Properties of lipid bilayer membranes separating two aqueous phases: composition studies. *J. Mol. Biol.* 31: 227.
72. Robertson, J. D. 1969. Molecular structure in biological membranes. In *Handbook of Molecular Cytology*. A. Lima-de-Faria, editor. North Holland Publishing Co., Amsterdam. 1403.